Modeling of Bubble Column Slurry Reactors for Multiple Reactions

A model of an isothermal bubble column slurry reactor for an arbitrary reaction network of R independent reactions and S reacting species has been developed. The model accounts for gas velocity variations due to a change in total number of moles during reaction, and for nonuniform catalyst distribution due to gravity settling. It is assumed that the gas phase is in plug flow and the batch liquid phase is unmixed, which is characteristic of pilot plant reactors with high aspect ratios. The minimum number of differential equations required for the complete description of the system is shown to be equal to the total number of independent reactions. A system of two series-parallel reactions, representative of Fischer-Tropsch synthesis, was used to study the effect of catalyst dispersion and model parameters on reactor performance. It was found that nonuniform catalyst distribution generally has a negative effect on conversion.

D. B. Bukur and W. H. Zimmerman
Kinetics, Catalysis and Reaction
Engineering Laboratory
Department of Chemical Engineering
Texas A&M University
College Station, TX 77843

Introduction

There has been considerable interest in the use of bubble column slurry reactors (BCSR) for biological reactions, direct coal liquefaction, the Fischer-Tropsch (F-T) synthesis, and hydrogenation reactions, among others (Deckwer et al., 1980; Ramachandran and Chaudhari, 1983). As a result, a number of studies have been concerned with the mathematical modeling aspects of BCSR. Most of these studies have considered the case where a single reaction is assumed to occur in the reactor, while the more general and interesting case of multiple reactions has not been investigated thoroughly.

An interesting feature of BCSR is the possibility of a nonuniform axial distribution of catalyst. This has been observed experimentally (Cova, 1966; Imafuku et al., 1968; Smith and Ruether, 1985), and it was found that the solid concentration profiles could be matched with a sedimentation-diffusion model (Cova, 1966; Kato et al., 1972). Recently, improvements in the calculations of the hindered settling velocity and the solids dispersion coefficient have been proposed by Smith and Ruether (1985), and a modification of the sedimentation-diffusion model for systems containing polydispersed solids has been presented by Smith et al. (1986).

The effect of nonuniform catalyst distribution on BCSR performance has been studied for the case of single first-order reaction by Govindrao and Chidambaram (1983), Kuo et al. (1983), and Stern et al. (1985). In all these studies it was found that the nonuniform catalyst distribution has a detrimental effect on the conversion. Recently, Bukur and Kumar (1986) have studied the effect of catalyst dispersion on conversion using two different types of reaction rate expressions, namely power law kinetics and Langmuir-Hinshelwood (L-H) kinetics. When power law kinetics were considered, lower conversions were predicted with the nonuniform catalyst distribution in comparison with conversions obtained assuming uniform catalyst distribution. However, with L-H kinetics it was found that enhancements in predicted values of conversion are possible for some values of model parameters in the presence of solids dispersion.

This work was undertaken with two main objectives:

1. To develop a general framework for analysis of a certain class of multiphase reaction systems with multiple reactions
2. To study the effect of nonuniform catalyst distribution on the performance of a BCSR with two series-parallel reactions that are representative of the F-T synthesis

A model that considers R independent chemical reactions involving S chemical species is developed for an isothermal, two-

phase steady-state reaction system based on the assumption that one phase (gas phase) is in plug flow and the second phase (liquid phase in a bubble column reactor, emulsion phase in a fluidized-bed reactor) is stationary and unmixed. Variations in the gas flow rate due to a change in total number of moles and in axial catalyst distribution due to gravity settling are also incorporated in the model. A model of this type is applicable, under certain conditions, to bubble column reactors for gas-liquid reactions or three-phase catalytic reactions, and also to fluid bed catalytic reactors. In particular, the assumptions made concerning the degree of mixing of the two phases are satisfactory for a BCSR with a high aspect ratio (say, $L/D > 40$), which is often the case with laboratory or pilot plant units.

Development of Model Equations

General model

The model equations in this work are developed assuming that:

1. The gas phase is in plug flow
2. The liquid phase is stationary and unmixed
3. There is a nonuniform axial distribution of catalyst within the reactor
4. Steady conditions exist and the reactor is operated at constant temperature and pressure
5. The dominant resistance to mass transfer is the liquid side of the gas-liquid interface
6. The slow reaction regime prevails

The system considered has S chemical species participating in R independent chemical reactions, where S is greater than R. The stoichiometry of the reactions may be represented as:

$$\boldsymbol{N}\boldsymbol{a} = 0 \tag{1}$$

where $\boldsymbol{N}$ is an $R \times S$ matrix of stoichiometric coefficients and $\boldsymbol{a}$ is an $S \times 1$ column vector of chemical species:

$$\boldsymbol{N} = \begin{pmatrix} \nu_{1,1} & \nu_{1,2} & \cdots & \nu_{1,S} \\ \nu_{2,1} & \nu_{2,2} & \cdots & \nu_{2,S} \\ \cdot & \cdot & & \cdot \\ \cdot & \cdot & & \cdot \\ \nu_{R,1} & \nu_{R,2} & \cdots & \nu_{R,S} \end{pmatrix} \quad \boldsymbol{a} = \begin{pmatrix} A_1 \\ A_2 \\ \cdot \\ \cdot \\ A_S \end{pmatrix} \tag{2}$$

The sign convention for stoichiometric coefficients followed is positive for products, negative for reactants, and zero if the species does not participate in a particular reaction.

The set of S gas phase mass balance equations can be represented in the form:

$$\frac{d}{dz}(U_G \boldsymbol{c}_G) = a_G \boldsymbol{K}_L (\boldsymbol{c}_L - \boldsymbol{c}_G^*) \tag{3}$$

$$(U_G \boldsymbol{c}_G)|_{z=0} = U_G^i \boldsymbol{c}_G^i \tag{3a}$$

where the $\boldsymbol{c}$ are $S \times 1$ column vectors of concentrations and $\boldsymbol{K}_L$ is an $S \times S$ diagonal matrix of mass transfer coefficients:

$$\boldsymbol{c}_G = \begin{pmatrix} C_{G,1} \\ C_{G,2} \\ \cdot \\ \cdot \\ C_{G,S} \end{pmatrix} \quad \boldsymbol{c}_G^* = \begin{pmatrix} C_{G,1}/m_1 \\ C_{G,2}/m_2 \\ \cdot \\ \cdot \\ C_{G,S}/m_S \end{pmatrix}$$

$$\boldsymbol{c}_G^i = \begin{pmatrix} C_{G,1}^i \\ C_{G,2}^i \\ \cdot \\ \cdot \\ C_{G,S}^i \end{pmatrix} \quad \boldsymbol{c}_L = \begin{pmatrix} C_{L,1} \\ C_{L,2} \\ \cdot \\ \cdot \\ C_{L,S} \end{pmatrix}$$

$$\boldsymbol{K}_L = \begin{pmatrix} k_{L,1} & 0 & 0 & \cdots & 0 \\ 0 & k_{L,2} & 0 & \cdots & 0 \\ \cdot & \cdot & \cdot & & \cdot \\ \cdot & \cdot & \cdot & & \cdot \\ 0 & 0 & 0 & \cdots & k_{L,S} \end{pmatrix} \tag{4}$$

In general, a net change in the total number of moles in the gas phase will occur with reaction, so the superficial gas velocity U_G will vary along the length of the reactor. An expression for the superficial gas velocity is obtained by summing Eq. 3 over all species:

$$C_G \frac{d}{dz}(U_G) = a_G \boldsymbol{u}^T \boldsymbol{K}_L (\boldsymbol{c}_L - \boldsymbol{c}_G^*) \tag{5}$$

$$U_G|_{z=0} = U_G^i \tag{5a}$$

where $\boldsymbol{u}^T$ is a $1 \times S$ row vector, $\boldsymbol{u}^T = (1 \quad 1 \quad \cdots \quad 1)$.

Also, the set of S liquid phase mass balances may be written as:

$$a_G \boldsymbol{K}_L (\boldsymbol{c}_L - \boldsymbol{c}_G^*) = \epsilon_L C_c \boldsymbol{N}^T \boldsymbol{r} \tag{6}$$

where $\boldsymbol{r}$ is an $R \times 1$ column vector of intrinsic reaction rates: $\boldsymbol{r} = (r_1 \quad r_2 \quad \cdots \quad r_R)^T$.

Equations 3–6 may be written in dimensionless form by introducing the following dimensionless groups and variables:

$$\begin{aligned} x_c &= C_c/C_{ca} & y_j &= C_{G,j}/C_{G,1}^i \\ x_j &= C_{L,j} m_j / C_{G,1}^i & N_{m,j} &= k_{L,j} a_G L / m_j U_G^i \\ d_j &= \epsilon_L L C_{ca} r_j / C_{G,1}^i U_G^i & v &= U_G/U_G^i \\ w_j &= y_j v & s &= z/L \end{aligned} \tag{7}$$

which leads to the following set of equations:

Gas Phase Mass Balance

$$\frac{d}{ds}(w) = N_m\left(x - \frac{1}{v}w\right) \tag{8}$$

$$w|_{s=0} = y^i \tag{8a}$$

Superficial Gas Velocity

$$\frac{d}{ds}(v) = \frac{1}{y_G}u^T N_m\left(x - \frac{1}{v}w\right) \tag{9}$$

$$v|_{s=0} = 1 \tag{9a}$$

Liquid Phase Mass Balance

$$N_m\left(x - \frac{1}{v}w\right) = x_c N^T d \tag{10}$$

where d is an $R \times 1$ column vector, w, x, and y^i are $S \times 1$ column vectors, and N_m is an $S \times S$ diagonal matrix, which have their components defined by Eq. 7.

The sedimentation-dispersion model of Kato *et al.* (1972) is used to describe the axial distribution of catalyst in the reactor. For a stationary liquid phase, the catalyst concentration is expressed as:

$$x_c = \frac{Pe_c}{1 - e^{-Pe_c}} e^{-Pe_c s} \tag{11}$$

With the model equations in this form, it is necessary to solve simultaneously $S + 1$ differential equations and S algebraic equations to obtain the concentration and velocity profiles; however, it is possible to reduce the number of differential equations to the number of independent chemical reactions, R. This reduction is always possible in homogeneous systems (Aris, 1965), but in multiphase systems the reduction is possible only in special cases. Bukur and Kumar (1986) have demonstrated this for the case of a single reaction occurring in a slurry bubble column with the same model as in this study. In the following development, the reduction is extended to the case of an arbitrary number of reactions and an arbitrary number of components. It will be shown that differential equations need only be solved for R key reacting species. With no loss of generality, the indexing of these species is chosen to run from 1 to R. The gas and liquid concentrations of the remaining $(S - R)$ subordinate species, indexed from $(R + 1)$ to S, and the superficial gas velocity, are algebraically related to the solutions for the key species.

By consideration of Eqs. 8 and 10, the gas phase mass balances may be rewritten in partitioned matrix form as:

$$(N_I|N_{II})^T d = \frac{1}{x_c}\frac{d}{ds}\begin{pmatrix} w_I \\ w_{II} \end{pmatrix} \tag{12}$$

where the N matrix has been partitioned into N_I, an $R \times R$ square matrix, and N_{II}, an $R \times (S - R)$ matrix, and the w vector has been partitioned into w_I, an $R \times 1$ column vector and w_{II}, an $(S - R) \times 1$ column vector:

$$N_I = \begin{pmatrix} \nu_{1,1} & \nu_{1,2} & \cdots & \nu_{1,R} \\ \nu_{2,1} & \nu_{2,2} & \cdots & \nu_{2,R} \\ \vdots & \vdots & & \vdots \\ \nu_{R,1} & \nu_{R,2} & \cdots & \nu_{R,R} \end{pmatrix} \quad w_I = \begin{pmatrix} w_1 \\ w_2 \\ \vdots \\ w_R \end{pmatrix}$$

$$N_{II} = \begin{pmatrix} \nu_{1,R+1} & \nu_{1,R+2} & \cdots & \nu_{1,S} \\ \nu_{2,R+1} & \nu_{2,R+2} & \cdots & \nu_{2,S} \\ \vdots & \vdots & & \vdots \\ \nu_{R,R+1} & \nu_{R,R+2} & \cdots & \nu_{R,S} \end{pmatrix} \quad w_{II} = \begin{pmatrix} w_{R+1} \\ w_{R+2} \\ \vdots \\ w_S \end{pmatrix} \tag{13}$$

The intrinsic reaction rates may be obtained by solving Eq. 12 in terms of the R key species:

$$d = \frac{1}{x_c}(N_I^T)^{-1}\frac{d}{ds}w_I \tag{14}$$

This relation is then used to eliminate the intrinsic reaction rates appearing in Eq. 12 for the subordinate species to obtain:

$$\frac{d}{ds}w_{II} = N_{II}^T(N_I^T)^{-1}\frac{d}{ds}w_I$$

$$= B\frac{d}{ds}w_I \tag{15}$$

where $B = N_{II}^T(N_I^T)^{-1}$ is an $(S - R) \times R$ matrix of constants related to the stoichiometric coefficients.

Equation 15 may be integrated directly to obtain a relationship between the R key species and the $(S - R)$ subordinate species:

$$w_{II} = y_{II}^i + B(w_I - y_I^i) \tag{16}$$

where the column vector y^i has been partitioned into y_I^i, an $R \times 1$ column vector for the key species, and y_{II}^i, an $(S - R) \times 1$ column vector for the subordinate species.

An expression for the velocity profile is obtained by consideration of Eqs. 8, 9, and 15. After manipulation, the dimensionless gas velocity may be expressed in terms of the R key species:

$$v = 1 + \frac{1}{y_G}e^T(w_I - y_I^i) \tag{17}$$

where e^T is a $1 \times R$ row vector of constants determined solely by stoichiometry:

$$e^T = (u_I^T + u_{II}^T B) \tag{18}$$

where u_I^T is an $R \times 1$ row vector, and u_{II}^T is an $(S - R) \times 1$ row vector obtained by the partitioning of u^T.

Equations 7 and 16 may be used to derive an expression for the gas phase concentrations of the $(S - R)$ subordinate spe-

cies:

$$y_{II} = \frac{y_{II}^i + \boldsymbol{B}\,(w_I - y_I^i)}{v} \tag{19}$$

where y_{II} is an $(S - R) \times 1$ column vector for the subordinate species. The velocity, v, is given by Eq. 17.

Finally, the liquid phase concentrations of the subordinate species are calculated considering Eqs. 8 and 15 to obtain:

$$N_{m,II}\, x_{II} = N_{m,II} y_{II} + \boldsymbol{B} N_{m,I}\left(x_I - \frac{1}{v} w_I\right) \tag{20}$$

where y_{II} is given by Eq. 19; $N_{m,I}$, is an $R \times R$ diagonal matrix, and $N_{m,II}$ is an $(S - R) \times (S - R)$ diagonal matrix, which are obtained by the partitioning of N_m. Similarly, the column vector x has been partitioned into x_I, an $R \times 1$ column vector for the key species, and x_{II}, an $(S - R) \times 1$ column vector for the subordinate species.

The original set of equations has been reduced with no loss of rigor to a set of R differential and R algebraic equations. The solutions for the superficial gas velocity and the gas and liquid concentrations of the $S - R$ subordinate species are given by Eqs. 17, 19, and 20, above. The remaining equations that must be solved to obtain the gas and liquid concentrations of the key species are:

Gas Phase Mass Balance

$$\frac{d}{ds}(w_I) = N_{m,I}\left(x_I - \frac{1}{v} w_I\right) \tag{21}$$

$$w_I|_{s=0} = y_I^i \tag{21a}$$

Liquid Phase Mass Balance

$$N_{m,I}\left(x_I - \frac{1}{v} w_I\right) = x_c N_I^T \boldsymbol{d}_I \tag{22}$$

where v is given by Eq. 17, and the gas phase concentrations of the key species are given by Eq. 7, $y_I = w_I/v$.

Single-reaction case

For the special case of a single reaction, the equations developed here for R reactions reduce to the equations presented by Bukur and Kumar (1986). All one needs to solve are the gas and the liquid phase mass balance equations, Eqs. 21–22, for one species only. The concentrations of all other species ($2 \rightarrow S$) and the variation of gas velocity can be expressed in terms of the single key species. It can be shown that the equations developed here for R reactions reduce to the equations presented by Bukur and Kumar.

Two-reaction example

The model equations developed for the multiple-reaction case have been applied to a system of two series-parallel reactions with five reacting species, representative of the Fischer-Tropsch synthesis. The two reactions considered are the F-T and water-gas shift (WGS) reactions, which may be written as:

$$\mathrm{CO} + (1 + m/2n)\mathrm{H_2} \rightarrow (1/n)\mathrm{C_nH_m} + \mathrm{H_2O} \quad \text{(F-T)} \tag{23}$$

$$\mathrm{CO} + \mathrm{H_2O} \rightleftharpoons \mathrm{H_2} + \mathrm{CO_2} \quad \text{(WGS)} \tag{24}$$

$\mathrm{C_nH_m}$ is used to model the hydrocarbon products of the F-T reaction. The reactions themselves will be indexed as: 1, F-T; and 2, WGS. Choosing $\mathrm{H_2}$ and CO to be the key species, the species will be indexed as: 1, $\mathrm{H_2}$; 2, CO; 3, $\mathrm{H_2O}$; 4, $\mathrm{CO_2}$; and 5, $\mathrm{C_nH_m}$. The stoichiometric matrix N is a 2×5 matrix given as:

$$N = \begin{bmatrix} -(1 + m/2n) & -1 & 1 & 0 & 1/n \\ 1 & -1 & -1 & 1 & 0 \end{bmatrix} \tag{25}$$

In this example, the $\boldsymbol{B}$ matrix is a 3×2 matrix, which is calculated from Eq. 15:

$$\boldsymbol{B} = \left(\frac{1}{2 + m/2n}\right)\begin{bmatrix} -2 & m/2n \\ 1 & -(1 + m/2n) \\ -1/n & -1/n \end{bmatrix} \tag{26}$$

The e^T vector needed for calculation of the dimensionless velocity is a 1×2 row vector which may be shown to be:

$$e^T = \left(\frac{1 + m/2n - 1/n}{2 + m/2n} \quad \frac{1 + m/2n - 1/n}{2 + m/2n}\right) \tag{27}$$

Defining $-\alpha = (1 + m/2n - 1/n)/(2 + m/2n)$, e^T may be rewritten as:

$$e^T = (-\alpha \quad -\alpha) \tag{28}$$

The gas velocity is determined from Eq. 17, which for the two-reaction case gives:

$$v = 1 - \frac{\alpha}{y_G}(w_1 - 1 + w_2 - y_2^i) \tag{29}$$

It is interesting to consider how the gas velocity varies with the combined $\mathrm{H_2}$ + CO conversion for this model. The $\mathrm{H_2}$ + CO conversion is defined as:

$$f_{1+2} = \frac{1 - w_1 + y_2^i - w_2}{1 + y_2^i} \tag{30}$$

Substitution into Eq. 29 yields:

$$v = 1 + \left(\frac{1 + y_2^i}{y_G}\right)\alpha f_{1+2} \tag{31}$$

This is an exact relationship, and shows that the velocity varies linearly with the $\mathrm{H_2}$ + CO conversion. In the typical case, the feed gas contains only $\mathrm{H_2}$ and CO, so that the term $(1 + y_2^i)/y_G = 1$. The value of α is a function only of the character of the hydrocarbon product, that is, stoichiometry, and can be determined *a priori* without solving the model equations. Well-defined limits may be placed on α by considering the extremes of product distribution, n, encountered in the F-T synthesis. When $n = 1$, methane is the only hydrocarbon product, and $m/n = 4$. Under these circumstances, α is $-\frac{1}{2}$. At the other extreme, when $n \rightarrow \infty$, $m/n \rightarrow 2$, and α is $-\frac{2}{3}$.

The gas phase concentrations of the subordinate species are obtained from Eq. 19, and in scalar form are given for any species k as:

$$y_k = \frac{y_k^i + B_{k-2,1}(w_1 - 1) + B_{k-2,2}(w_2 - y_2^i)}{v} \qquad k = 3 \rightarrow 5 \quad (32)$$

where v has been previously determined by either Eq. 29 or Eq. 31.

The liquid phase concentrations of species 3–5 are obtained from Eq. 20, and may also be expressed in scalar form:

$$x_k = y_k + B_{k-2,1}\frac{N_{m,1}}{N_{m,k}}\left(x_1 - \frac{1}{v}w_1\right) + B_{k-2,2}\frac{N_{m,2}}{N_{m,k}}\left(x_2 - \frac{1}{v}w_2\right) \qquad k = 3 \rightarrow 5 \quad (33)$$

where y_k is known from Eq. 32.

The variables w_1, w_2, x_1, and x_2 are obtained by solving the gas and liquid mass balances simultaneously for H_2 and CO, which are given as:

Gas Phase Mass Balance

$$\frac{d}{ds}(w_j) = N_{m,j}\left(x_j - \frac{1}{v}w_j\right) \qquad j = 1, 2 \quad (34)$$

$$w_j|_{s=0} = y_j^i \qquad j = 1, 2 \quad (34a)$$

Liquid Phase Mass Balance

$$N_{m,j}\left(x_j - \frac{1}{v}w_j\right) = x_c(\nu_{1,j}d_1 + \nu_{2,j}d_2) \qquad j = 1, 2 \quad (35)$$

where the gas phase concentrations of the key species are obtained from Eq. 7, $y_j = w_j/v$, $j = 1, 2$.

Under conditions of fast mass transfer (FMT), some simplifications of the model equations can be made. As $N_{m,j} \rightarrow \infty$, x_j and y_j become equal, i.e., the gas and liquid phase are in equilibrium. Then the gas phase mass balance becomes:

$$\frac{d}{ds}(w_j) = x_c(\nu_{1,j}d_1 + \nu_{2,j}d_2) \qquad j = 1, 2 \quad (36)$$

where reaction rates, d_i, are now evaluated using gas phase concentrations. The previous results for gas velocity, Eq. 29 or 31, and the relations for the gas phase concentrations of the three subordinate species, Eq. 32, are still valid.

The two-reaction model was applied using the L-H kinetics of Leib and Kuo (1984) for the F-T and WGS reactions. In dimensionless form, the rate expressions are:

$$d_1 = \frac{\lambda_1 x_1 x_2}{x_2 + \lambda_3 x_3} \quad (37)$$

$$d_2 = \frac{\lambda_2(x_2 x_3 - x_1 x_4/\lambda_4)}{x_2 + \lambda_3 x_3} \quad (38)$$

where the dimensionless reaction numbers have been defined as:

$$\lambda_1 = \epsilon_L LC_{ca}k_1/m_1U_G^i \quad \lambda_2 = \epsilon_L LC_{ca}k_2/m_3U_G^i$$
$$\lambda_3 = m_2k_3/m_3 \quad \lambda_4 = m_1m_4k_4/m_2m_3 \quad (39)$$

Leib and Kuo have also developed a two-reaction BCSR model for the F-T synthesis that is essentially the same as the two-reaction example considered here. They assumed that the gas phase was in plug flow, the liquid phase was unmixed, and that a nonuniform catalyst distribution could develop in the reactor. Both the F-T and WGS reactions were considered to occur simultaneously, with the stoichiometry of the F-T reaction given by:

$$CO + (1 + m/2)H_2 \rightarrow (\text{—}CH_m\text{—}) + H_2O \quad (40)$$

A linear variation of gas velocity with H_2 + CO conversion was assumed on the basis of experimental observation that the volume contraction is a linear function of conversion. Values of contraction parameter α of -0.5 and -0.62 were employed in their calculations. Four differential gas phase balances and four algebraic liquid phase balances were solved simultaneously to obtain H_2, CO, H_2O, and CO_2 gas and liquid phase concentration profiles. Since the hydrocarbon product produced during reaction does not appear in the reaction rate expressions, the mass balance equations for this species were not formulated and consequently its concentration profiles were not obtained. Finally, they considered a very small catalyst particle diameter, 3 μm, which with their other parameter values leads to an essentially uniform catalyst distribution in the reactor. The results of their model calculations were in good agreement with experimental data obtained in a 0.05 m ID × 7.62 m tall pilot reactor operated by Mobil, which indicates that models of this type are useful for describing the behavior of actual reactors.

The theory developed in this study provides justification for the observed linear dependence of gas velocity on conversion, Eq. 31, and relates the contraction parameter to reaction stoichiometry, Eq. 28. Also, this theory leads to reduction in computations required (two differential equations only). Aside from these fundamental differences the model used here is identical to the model developed by Leib and Kuo.

Stern *et al.* (1985) have also studied the same type of BCSR model where the F-T and WGS reactions occur simultaneously. The stoichiometry of the F-T reaction was similar to that used here, except that they chose to express the stoichiometric coefficients in terms of the Schulz-Flory chain growth probability factor and the overall C_2^+ paraffin fraction of the hydrocarbon product. The mass balance equations for all five species plus the overall gas balance were solved simultaneously to obtain the reactant conversion and concentration profiles in both phases.

Stern *et al.* studied the effect of a nonuniform catalyst distribution on conversion using a model that considered dispersion in all three phases, which simplifies to the unmixed model when the gas and liquid phase Peclet numbers approach infinity. They found that catalyst dispersion has a negative effect on catalyst performance when mass transfer influences the reaction rates. The calculations with nonuniform catalyst distribution were made only for the case of a single reaction following first-order kinetics. The unmixed model with a uniform catalyst distribution was used to compare model predictions with the experimen-

tal data of Deckwer *et al.* (1982) and Kuo *et al.* (1983). The simple first-order kinetics for the F-T synthesis reaction were again used for all but one case, while the WGS reaction was assumed to follow mass action kinetics. The rate constants were obtained by fitting the model to a single experimental data point, and the model was allowed to predict performance at other conditions. In most cases the model predictions were in good agreement with the experimental data.

Numerical Methods

When the mass transfer numbers are finite, the gas and liquid mass balances, Eqs. 34–35, must be solved simultaneously. A Runge-Kutta technique was used to integrate Eq. 34 for H_2 and CO. At each step of the integration it was necessary to solve the liquid phase mass balances iteratively using a Newton-Raphson method. The objective functions for the Newton-Raphson method are the liquid phase mass balances for H_2 and CO, which were arranged to have the form:

$$Q_j(s, w_1, w_2) = 0; \quad j = 1, 2 \tag{41}$$

The procedure for solving the model equations begins at the reactor inlet, where the liquid phase concentrations of H_2 and CO are calculated by solving Eq. 41. The liquid phase concentrations of the subordinate species are then calculated using Eq. 33. An incremental step in position is taken, and the liquid concentrations are again calculated given w_1 and w_2; the gas velocity is calculated using Eq. 29, and the subordinate gas phase concentrations are calculated using Eq. 32. The gas phase mass balances are solved, and the position is incremented. The process is repeated until the end of the reactor is reached. The same solution procedure is used for the case of fast mass transfer, except that an iterative solution is not needed to obtain the liquid phase concentrations of H_2 and CO.

Model Parameters

The base case conditions were selected to represent the operation of the laboratory plant described by Kölbel and Ralek (1980) in order to arrive at realistic values for the model parameters; they are summarized in Table 1. The solubility of the hydrocarbon product was estimated using the correlation of Hayduk and Cheng (1970) for propylene and its diffusivity was estimated from the Wilke-Chang correlation. The solubilities and diffusivities of the remaining species were obtained from the relations reported by Kuo et al. (1983) and Leib and Kuo (1984). The correlation of Calderbank and Moo-Young (1961) was used to calculate mass transfer coefficients. The density and viscosity of the liquid were obtained from Deckwer et al. (1980), and their correlations were used to determine the gas holdup and gas-liquid interfacial area. An average value of gas velocity, based on a H_2 + CO conversion of 88%, was used to evaluate the gas holdup and interfacial area. The kinetic parameters in the reaction rate expressions were estimated from values given by Leib and Kuo (1984).

The catalyst Peclet number was allowed to vary between 0 and 5. The case of a Peclet number equal to zero corresponds to a uniformly distributed catalyst, and the gradient becomes more severe as the Peclet number increases. The Peclet number is strongly dependent on the catalyst particle size and density and the reactor geometry. Large Peclet numbers are possible even with relatively small particles. For example, the Peclet number, determined from the correlations of Kato et al. (1972), for Mobil's pilot plant reactor with 15 wt. % slurry of iron oxide catalyst particles 50 μm in diameter and a density of 2,100 kg/m^3 is 4.4.

Table 1. Model Parameters and Values Used in Base Case Calculations

Reactor diameter	0.047 m
Effective slurry bed height	3.5 m
Superficial gas velocity at inlet	0.035 m/s
Molar H_2/CO feed ratio	0.67
Average hydrocarbon chain length	3
Average hydrocarbon H/C ratio	2.2
Average liquid hold-up	0.84
Gas contraction parameter	−0.57
Average catalyst concentration	110 kg cat/m^3 liq
Mass transfer numbers $N_{m,1} - N_{m,5}$	9.4, 3.3, 14, 6.4, 7.1
Constants in rate expressions	$k_1 = 1.4 \times 10^{-3}$ m^3 liq/kg cat · s $k_2 = 1.0 \times 10^{-3}$ m^3 liq/kg cat · s $k_3 = 0.76$ $k_4 = 34.9$
Reaction numbers λ_1–λ_4	2.8, 7.9, 2.4, 63
Species indexing	1, H_2; 2, CO; 3, H_2O; 4, CO_2; 5, C_nH_m

Results and Discussion

Parameter variations were made in order to study the behavior of the two-reaction system and the effect of catalyst dispersion on reactor performance. The parametric study was conducted by varying only one parameter at a time, holding all remaining parameters constant. The range of parameters considered was chosen to clearly show trends in reactor performance. Another situation considered is the case of fast mass transfer (FMT) between the gas and liquid phases. Under these conditions, the gas and liquid concentrations of all species are in physical equilibrium at each point in the reactor.

The effect of catalyst dispersion on the H_2 + CO conversion profiles for the base case is shown in Figure 1. Under the base case conditions the reaction rates are decreasing over all or most of the reactor length, Figure 2, as is the catalyst concentration, and thus the exit conversion decreases as the catalyst distribution becomes more nonuniform. The detrimental effect of nonuniform catalyst distribution on H_2 + CO conversion was observed in Mobil's pilot plant reactor in runs 9, 11, and 13. Kuo et al. (1985) reported a drop in conversion and development of a nonuniform axial temperature profile as a consequence of the catalyst settling, which was most likely caused by agglomeration of catalyst particles.

Internally, there may be regions where the conversion for a dispersed catalyst is higher than for a uniformly distributed catalyst, however, due to mass transfer effects the overall utilization of catalyst is diminished and the efficiency of the reactor decreases. When there are no mass transfer limitations (FMT), the reactor performance is independent of catalyst dispersion and the conversion is determined solely by the amount of catalyst present in the reactor. The exit conversion in this case is

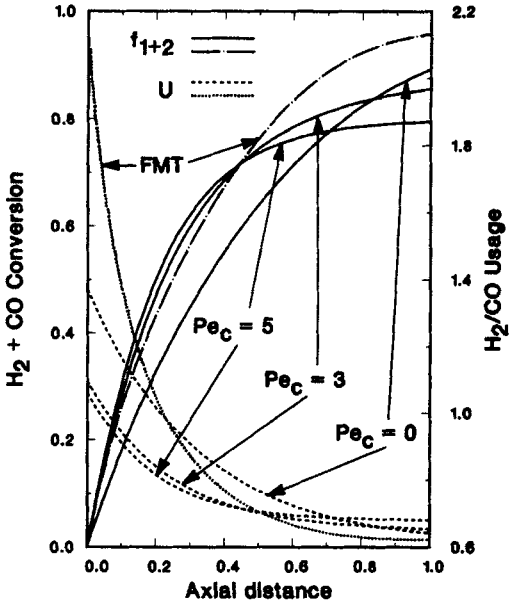

Figure 1. Effect of catalyst dispersion on H_2 + CO conversion and H_2/CO usage profiles for base case and fast mass transfer case.

greater than in the presence of gas-liquid mass transfer resistances.

The H_2/CO usage profiles are also shown in Figure 1. Usage is defined to be the amount of H_2 consumed over the amount of CO consumed; it can be calculated from:

$$U = F\frac{f_1}{f_2} \tag{42}$$

By considering the extremes for the WGS, the limits on possible values for the usage ratio are $(m/4n) < U < (1 + m/2n)$.

The maximum utilization of the feed gas is governed by the usage. Only when the usage equals the feed ratio will the utilization of the feed be maximized. This may be seen by considering the following relations:

$$f_{1+2} = \frac{F(1+U)}{U(1+F)}f_1 = \frac{(1+U)}{(1+F)}f_2 \tag{43}$$

The usage decreases with distance for all values of catalyst Peclet number, and over a large portion of the reactor it is greater than the feed ratio. This can be explained by the fact that initially the rate of the F-T reaction is greater than the rate of the WGS reaction, but as the former decreases more rapidly than the latter, the usage decreases continuously along the bed. At the reactor exit $U < F$ for $Pe_c = 0$ and 3, as well as for the fast mass transfer case, but $U > F$ for $Pe_c = 5$.

The effect of axial catalyst distribution on the reaction rates may be seen in Figure 2, where the reaction rate profiles of the F-T and WGS reactions are plotted for catalyst Peclet numbers of 0, 3, and 5. The rate of the F-T reaction decreases steadily throughout the reactor, whereas the rate of the WGS reaction passes through a maximum. In the inlet region of the reactor, the reaction rates for a dispersed catalyst are higher than for a uniformly distributed catalyst because of the higher catalyst concentration; however, due to mass transfer limitations the utilization of catalyst is lower. The rates diminish quickly with reactor length and approach zero in the exit region of the reactor because of low catalyst and reactant concentrations.

The effect of the reaction numbers λ_1 and λ_2 on the H_2 + CO conversion is given in Figure 3 for catalyst Peclet numbers of 0 and 5. The rate of the F-T reaction is governed by λ_1, and the rate of the WGS reaction is governed by λ_2. As λ_1 is increased above zero, the H_2 + CO conversion increases rapidly until an asymptotic value is reached as the reaction becomes reactant-

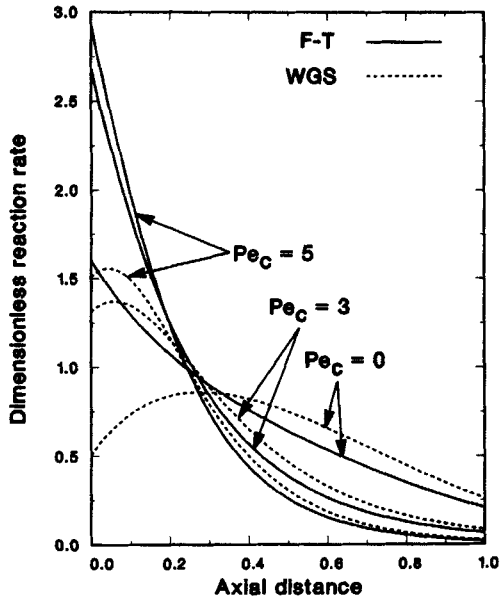

Figure 2. Effect of catalyst dispersion on reaction rate profiles for Fischer-Tropsch and water-gas shift reactions.

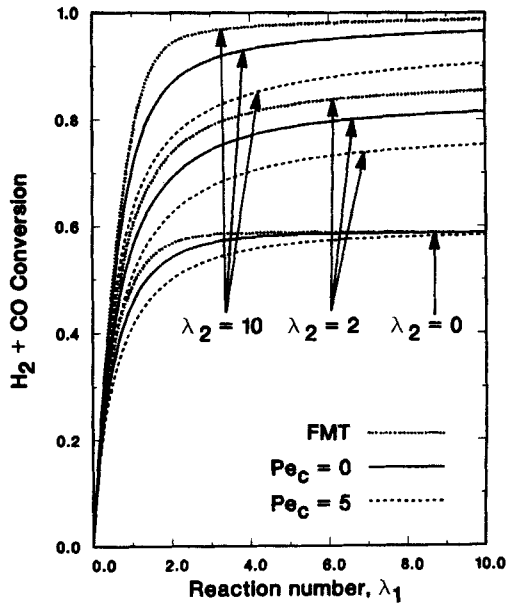

Figure 3. Effect of reaction numbers λ_1 and λ_2 on H_2 + CO conversion.

limited. Since the feed ratio is fixed, the asymptotic value attained is determined by the ultimate usage ratio. When λ_2 is zero the rate of the water gas shift is zero, so the usage is given by $(1 + m/2n)$. In this case the usage ratio (2.1) is much greater than the H_2/CO feed ratio (0.67) and hydrogen is the limiting reactant. The limiting value of H_2 + CO conversion is given by Eq. 43 with $f_1 = 1$. As λ_2 is increased, the WGS reaction produces H_2 from the CO-rich feed and lowers the usage toward the feed ratio, increasing the asymptotic value of the conversion.

The effect of catalyst dispersion and mass transfer may also be seen in Figure 3. The conversions obtained with a nonuniform catalyst distribution are generally less than with a uniformly distributed catalyst, and the difference is greater at the larger values of λ_2, while the difference is less at the larger values of λ_1. This may be attributed to the amount of reactor space required to reach the ultimate conversion. At high values of λ_1, with fast mass transfer, only the inlet region of the reactor is needed before the reaction becomes reactant limited, and further increases in λ_1 will not alter the ultimate value of conversion appreciably. With finite mass transfer, more reactor space and higher values of λ_1 are needed to reach the ultimate value of conversion.

The effect of the reaction numbers λ_3 and λ_4 on the H_2 + CO conversion is given in Figure 4 for catalyst Peclet numbers of 0 and 5. The adsorption parameter of H_2O and thus product inhibition is governed by λ_3. The equilibrium of the WGS reaction is governed by λ_4, where high values of λ_4 drive the reaction to the right, favoring the production of H_2 and CO_2. The effect of product inhibition by water is clearly seen as the conversion decreases with increasing λ_3. High values of λ_4 increase the conversion in this particular case of a low feed ratio because high values of λ_4 favor the shift toward H_2, bringing the usage closer to the feed ratio. Conversion decreases substantially due to mass transfer resistances and nonuniform catalyst distribution.

Figures 5 and 6 show the effect of varying the mass transfer numbers on the H_2 + CO conversion with the catalyst Peclet

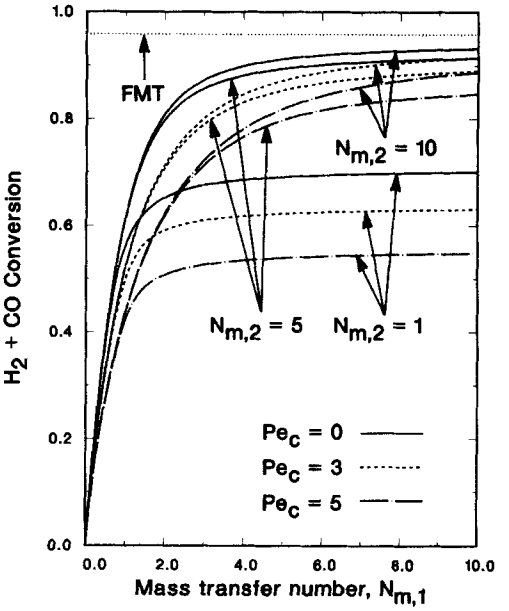

Figure 5. Effect of mass transfer numbers of H_2 and CO on H_2 + CO conversion.

number as a parameter. The mass transfer numbers may be varied independently by varying the corresponding mass transfer coefficient. From a physical perspective, this amounts to varying the estimate of the liquid diffusivity of the species.

The effect of the mass transfer numbers of the reactants, H_2 and CO, on the conversion is given in Figure 5. The conversion for the uniformly distributed catalyst is higher than for the dispersed catalyst, as before. Also, it is observed that the difference in conversion decreases as the mass transfer number increases. This is expected since faster mass transfer lessens the negative effect of nonuniform catalyst distribution on conversion by

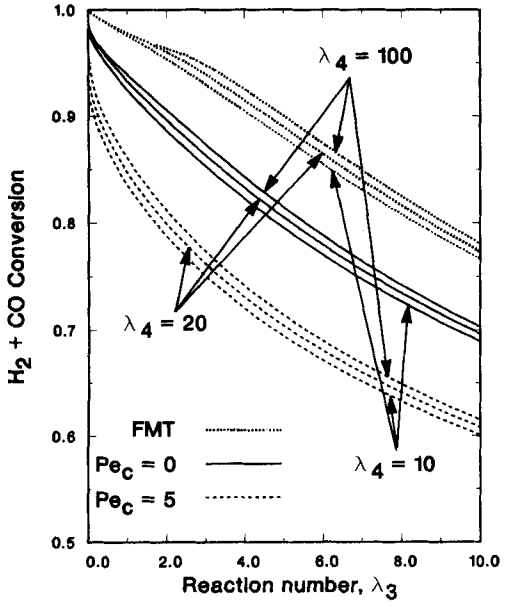

Figure 4. Effect of reaction numbers λ_3 and λ_4 on H_2 + CO conversion.

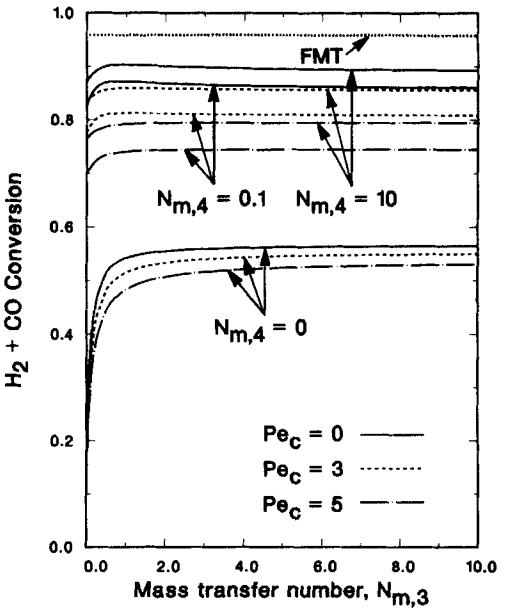

Figure 6. Effect of mass transfer numbers of H_2O and CO_2 on H_2 + CO conversion.

improving the utilization of the catalyst in the lower regions of the reactor where the catalyst concentration is high. The conversion corresponding to the infinite rate of mass transfer (FMT) is also shown in Figure 5 for comparison.

The effect of the mass transfer numbers of products, H_2O and CO_2, on conversion is shown in Figure 6. For products, a mass transfer number of zero means that all of the product formed remains in the liquid phase. At low values of $N_{m,3}$, the H_2O concentration in the liquid phase increases, which decreases the reaction rates and hence conversion because of product inhibition. Values of $N_{m,3}$ greater than 2 have little effect on the conversion, which indicates that other processes are much slower than the mass transfer of water. A similar increase in the liquid phase concentration of CO_2 ($N_{m,4} = 0$) also leads to low conversions. High CO_2 concentration drives the WGS reaction toward CO, increasing the usage and thus lowering the H_2 + CO conversions obtained. This effect is limited only to very low values of $N_{m,4}$, as can be seen by comparing results for $N_{m,4} = 0.1$ and 10.

Figure 7 shows the effect of the H_2/CO molar feed ratio on both the H_2 + CO conversion and usage. The molar feed ratio was allowed to vary between 0.5 and 2, which is a range of values typical of those encountered in the F-T synthesis. The conversions pass through a maximum at a feed ratio of about 0.7, which corresponds to the region where the usage and feed ratios are approximately equal for catalysts with significant WGS activity. The effect of the H_2/CO feed ratio is studied further in Figure 8. In this figure, the effect of the reaction number λ_1 on conversion is shown with the feed ratio as a parameter. In this way, the effect of the feed ratio at different conversion levels may be studied. it is observed that at high conversions (higher λ_1) the optimum feed ratio is 0.67. At lower conversions the optimum H_2/CO feed ratio shifts toward higher values. Thus, the optimum value of the feed ratio appears to be largely determined by the level of conversion and catalyst activity for the WGS reaction.

These model predictions are in qualitative agreement with experimental results reported in the literature. Deckwer et al.

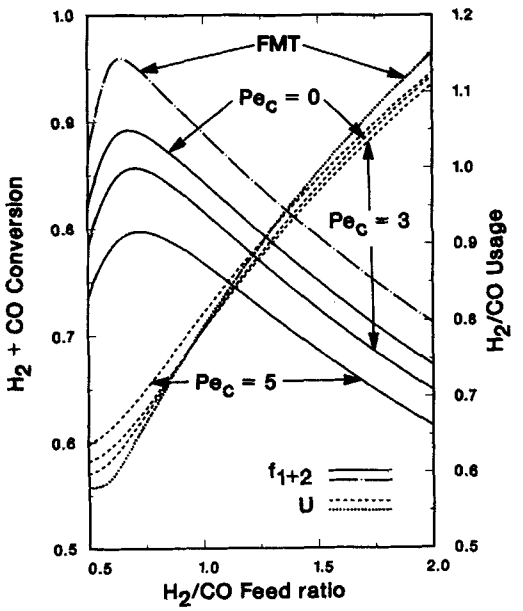

Figure 7. Effect of H_2/CO feed ratio on H_2 + CO conversion and H_2/CO usage.

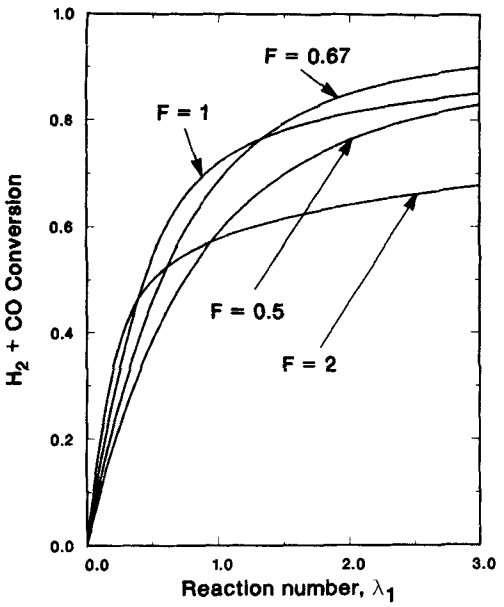

Figure 8. Effect of reaction number λ_1 and feed composition on H_2 + CO conversion.

(1982) found that the maximum H_2 + CO conversion is obtained with H_2/CO feed ratios between 0.6 and 0.7 in experiments with Fe/Mn catalyst in a 0.038 m ID, 2 m tall slurry bubble column reactor. The existence of maximum in conversion for feed ratios between 0.7 and 0.8 was also observed in our laboratory in experiments with fused iron catalyst in a stirred tank slurry reactor (Buck, 1986). It should be noted that in both the Rheinpreussen demonstration plant (Kölbel and Ralek, 1980) and Mobil's pilot plant (Kuo et al., 1983, 1985) the synthesis gas with H_2/CO molar ratio of 0.67 was used. This value is close to the optimum predicted by the model. Also the model prediction that the optimum H_2/CO feed ratio at lower conversions shifts toward higher values is in qualitative agreement with experimental results obtained in our laboratory (Bukur and Brown, 1986).

Conclusions

A model for a bubble column slurry reactor has been developed that allows for an arbitrary number of chemical reactions, and that accounts for a nonuniform axial catalyst distribution and variation of gas velocity with a change in total number of moles. It is assumed that the gas phase is in plug flow and that the batch liquid phase is unmixed, which is characteristic of reactors with a high aspect ratio. It is shown that only a minimum number of differential equations for certain key species need to be solved. This minimum number of equations is equal to the number of independent chemical reactions occurring in the system. The general theoretical framework developed in this paper is also applicable, under certain conditions, to bubble column reactors for gas-liquid reactions, and to fluid bed catalytic reactors (negligible gas flow through the dense phase).

The model has been applied to a system in which two series-parallel reactions occur, and were chosen to represent the Fischer-Tropsch synthesis. It was found that as the catalyst distribution becomes more nonuniform, the combined H_2 + CO conversion decreases in all cases. The most important mass transfer

resistance is for CO. The base value of the mass transfer number for H_2 is high, and consequently its mass transfer resistance is small. The mass transfer rates of products have a very small effect on predictions of H_2 + CO conversions, except when they are much smaller than in the base case. The optimum feed ratio for a given catalyst varies with conversion and with the catalyst activity toward the WGS reaction. For the base case, the maximum utilization of the synthesis gas can be achieved with a CO-rich feed gas (F = 0.6–0.7), since in this case the usage ratio approaches the H_2/CO feed ratio. The model predictions are sensitive to changes in the kinetic parameters and their values are subject to a great deal of uncertainty.

Acknowledgment

This work was partially supported by the Center for Energy and Mineral Resources at Texas A&M University.

Notation

a_G = interfacial area, m^2 liquid/m^3
C_c = catalyst concentration, kg catalyst/m^3 liquid
C_{ce} = average catalyst concentration, kg catalyst/m^3 liquid
C_G = total gas phase concentration, mol/m^3 gas
$C_{G,j}$ = gas phase concentration of species j, $j = 1 \rightarrow S$, mol/m^3 gas
$C^*_{G,j}$ = equilibrium liquid phase concentration of species j, $j = 1 \rightarrow S$, mol/m^3 liquid
$C_{L,j}$ = liquid phase concentration of species j, $j = 1 \rightarrow S$, mol/m^3 liquid
d_i = intrinsic reaction rate of reaction i, $i = 1 \rightarrow R$, Eq. 7
f_j = fractional conversion of species j, $j = 1 \rightarrow S$
f_{1+2} = combined H_2 + CO fractional conversion
F = molar H_2/CO feed ratio
$k_{L,j}$ = mass transfer coefficient of species j, $j = 1 \rightarrow S$, m liquid/s
L = effective length of slurry bed, m
m = average number of hydrogen atoms per molecule of synthesis product
m_j = solubility coefficient of species j, $j = 1 \rightarrow S$, m^3 liquid/m^3 gas
n = average number of carbon atoms per molecule of synthesis product
$N_{m,j}$ = mass transfer number of species j, $j = 1 \rightarrow S$, Eq. 7
Pe_c = catalyst Peclet number
Q = value of objective function for liquid phase mass balances
r_i = intrinsic rate of reaction i, mol/kg catalyst · s
R = total number of independent reactions
s = distance, Eq. 7
S = total number of chemical species
U = H_2/CO usage ratio
U_G = superficial gas velocity, m/s
v = superficial gas velocity, Eq. 7
w_j = molar flux of species j, $j = 1 \rightarrow S$, Eq. 7
x_c = catalyst concentration, Eq. 7
x_j = liquid phase concentration of species j, $j = 1 \rightarrow S$, Eq. 7
y_G = total gas phase concentration, $y_G = C_G/C^i_{G,1}$
y_j = gas phase concentration of species j, $j = 1 \rightarrow S$, Eq. 7
z = axial position in slurry bed, m

Greek letters

α = gas contraction parameter, Eq. 28
ϵ_L = liquid holdup, m^3 liquid/m^3
λ = reaction number, Eq. 39
$\nu_{i,j}$ = stoichiometric coefficient of species j in reaction i, $j = 1 \rightarrow S$, $i = 1 \rightarrow R$

Subscripts

I = matrix or vector partitioned for R key species
II = matrix or vector partitioned for $S - R$ subordinate species
G = gas phase
i = reaction, $i = 1 \rightarrow R$
j = any species, $j = 1 \rightarrow S$
k = subordinate species, $k = (R + 1) \rightarrow S$
L = liquid phase

Superscripts

i = inlet value
T = transpose of matrix or vector

Literature cited

Aris, R., *Introduction to the Analysis of Chemical Reactors,* Prentice-Hall, Englewood Cliffs, NJ (1965).

Buck, H. J., "Fischer-Tropsch Synthesis Over a Fused Iron Catalyst in a Three-Phase Slurry Reactor," M.S. Thesis, Texas A&M Univ. (1986).

Bukur, D. B., and R. F. Brown, "Fischer-Tropsch Synthesis in a Stirred Tank Slurry Reactor—Reaction Rates," *Can. J. Chem. Eng.,* (1986).

Bukur, D. B., and V. R. Kumar, "Effect of Catalyst Dispersion on Performance of Slurry Bubble Column Reactors," *Chem. Eng. Sci.,* **41,** 1435 (1986); (accepted for publication).

Calderbank, P. H., and M. B. Moo-Young, "The Continuous Phase Heat and Mass Transfer Properties of Dispersions," *Chem. Eng. Sci.,* **16,** 39 (1961).

Cova, D. R., "Catalyst Suspension in Gas-Agitated Tubular Reactors," *Ind. Eng. Chem. Process Des. Dev.,* **5,** 20 (1966).

Deckwer, W.-D., Y. Louisi, A. Zaidi, and M. Ralek, "Hydrodynamic Properties of the Fischer-Tropsch Slurry Process," *Ind. Eng. Chem. Process Des. Dev.,* **19,** 699 (1980).

Deckwer, W.-D., Y. Serpemen, M. Ralek, and B. Schmidt, "Fischer-Tropsch Synthesis in the Slurry Phase on Mn/Fe Catalysts," *Ind. Eng. Chem. Process Des. Dev.,* **21,** 222 (1982).

Govindrao, V. M. H., and M. Chidambaram, "On the Steady-State Performance of Cocurrent Bubble Column Slurry Reactors," *Chem. Eng. J.,* **27,** 29 (1983).

Hayduk, W., and S. C. Cheng, "Solubilities of Ethane and Other Gases in Normal Paraffin Solvents," *Can. J. Chem. Eng.,* **48,** 93 (1970).

Imafuku, K., T. Y. Wang, K. Koide, and H. Kubota, "Behavior of Suspended Solid Particles in a Bubble Column," *J. Chem. Eng. Jap.,* **21,** 153 (1968).

Kato, Y., A. Nishiwaki, T. Fukuda, and S. Tanaka, "The Behavior of Suspended Solid Particles and Liquid in Bubble Columns," *J. Chem. Eng. Jap.,* **5,** 112 (1972).

Kölbel, H., and M. Ralek, "The Fischer-Tropsch Synthesis in the Liquid Phase," *Catal. Rev. Sci. Eng.,* **21,** 225 (1980).

Kuo, J. C. W., et al., "Slurry Fischer-Tropsch/Mobil Two-Stage Process of Converting Syngas to High Octane Gasoline," Final Report to U.S. Dept. of Energy, Contract No. DE-AC22-80PC30022 (1983).

———, "Two-Stage Process for Conversion of Synthesis Gas to High-Quality Transportation Fuels," Final Report to U.S. Dept. of Energy, Contract No. DE-AC22-83PC60019 (1985).

Leib, T. M., and J. C. W. Kuo, "Modeling the Fischer-Tropsch Synthesis in Slurry Bubble-Column Reactors," *AIChE Ann. Meet.,* San Francisco (Nov., 1984).

Ramachandran, P. A., and R. V. Chaudhari, *Three-Phase Catalytic Reactors,* Gordon and Breach, New York (1983).

Smith, D. N., and J. A. Ruether, "Dispersed Solid Dynamics in a Slurry Bubble Column," *Chem. Eng. Sci.,* **40,** 741 (1985).

Smith, D. N., J. A. Ruether, Y. T. Shah, and M. N. Badgujar, "Modified Sedimentation-Dispersion Model for Solids in a Three-Phase Slurry Column," *AIChE J.,* **32,** 426 (1986).

Stern, D., A. T. Bell, and H. Heinemann, "A Theoretical Model for the Performance of Bubble-Column Reactors Used for Fischer-Tropsch Synthesis," *Chem. Eng. Sci.,* **40,** 1665 (1985).

Manuscript received Oct. 8, 1986, and revision received Jan. 13, 1987.